Assessment of modal density and free path distribution in central-planned halls

Published Version:
Fratoni, G., Garai, M., D'Orazio, D. (2023). Assessment of modal density and free path distribution in central-planned halls. THE JOURNAL OF THE ACOUSTICAL SOCIETY OF AMERICA, 154(6), 3604-3614 [10.1121/10.0022569].

Availability:
This version is available at: https://hdl.handle.net/11585/951854 since: 2024-01-03

Published:
DOI: http://doi.org/10.1121/10.0022569

Assessment of modal density and free path distribution in central-planned halls

Giulia Fratoni, Massimo Garai, and Dario D'Orazio

Department of Industrial Engineering, University of Bologna,Viale Risorgimento 2, Bologna, 40136, Italy[a]

Central-planned halls are highly widespread in the historical architectures of the Western world, such as rotundae, Christian baptisteries, and Roman tombs. In such halls, whispering galleries, flutter echoes, and sound focusing are the acoustic phenomena mainly investigated by scholars. Instead, modal behaviour and free path distribution are generally less treated in literature. The present study explores the modal density at low frequencies and the relationship with the most recurrent free path lengths in three historical nearly circular spaces, here assessed as case studies. Acoustic measurements allowed the collection of objective experimental data, i.e., room impulse responses and the resulting room acoustics criteria. Wave-based numerical models allowed investigating the eigenfrequencies distribution, whilst the free paths trend has been experienced through ray-based models. The main outcomes of both analyses show the prominence of the circular modes, rather than the diametral and the elevation ones. Moreover, the mean free path calculated using ray-tracing proves to be higher than the theoretical value commonly assumed for any kind of shape. The consequent longer reverberations compared to halls with other shapes and the same volume justify the significant support historically provided to sound signals by circular halls.

[a]dario.dorazio@unibo.it

I. INTRODUCTION

Among the first scientific studies on circular spaces dating back to the 1920s, one notable insight is provided by W. C. Sabine – the founder of architectural acoustics as a science – who analysed the domes of St. Paul Cathedral in London and the Hall of Statues of the U.S. Capitol in Washington D.C. (Sabine, 1922). The former hall is known for the *whispering galleries* effect: a phenomenon due to rigid boundaries (hard walls), a low sound power level of the sound source, and grazing incidence between the sound source and the walls (Bate, 1938). The same role of hard walls was confirmed when the dome of the Hall of Statues of the U.S. Capitol was restored after a fire and some painted coffers were replaced by plaster coffers with cavities. After the restoration, the focusing effect noted by Sabine was unintentionally reduced due to the diffuse reflections (Cremer and Müller, 1978). Another phenomenon that is generally investigated in circular environments is related to *focusing effects*. The first insights on such a topic dated back to Kircher's Phonurgia nova (Kircher, 1673), who studied proto-wave guides. The sound rays analogy was well known by scholars since the 17^{th} Century (D. D'Orazio, 2019). Focusing effects were corrected by Meyer and Kuttruff by placing suspended ceilings inside the Festival Hall of the Farbwerke Hoechst, and by Reichardt et al. using reflecting ceilings in the Haus del Lehrers (Meyer, 1964; Reichardt, 1968). A further acoustic effect typically studied in circular spaces is the *flutter echo*. In the presence of domes, flutter echoes are regularly repeated over time (Alberdi *et al.*, 2019; Magrini and Ricciardi, 2006). This often happens in central-planned curved architectures, which have time-aligned geometric reflections due to the smoothness of reflective surfaces and the lack of scattering elements. With this regard, a large number of studies were focused on Orthodox churches and mosques, due to their typical geometries (Kosała and Małecki, 2018; Shepherd *et al.*, 2005; Sü Gül *et al.*, 2016). Generally, since the 1930s scholars have been investigating flutter echoes in the case of concave surfaces, such as domes, where the reflection may be significantly increased and heard separately from the direct sound (Petzold, 1930). Further research allowed to define the first analytic treatments on flutter echo, proposing the taxonomy in four categories, depending on the vault curvature and the specific superposition of acoustic rays (Haas, 1951; Maa, 1941; Muncey *et al.*, 1953). Later, scholars studied the cancellation of echo phenomena in Cabanchel Boxing Pavillion (Madrid) by using ray tracing techniques (Moreno *et al.*, 1981). Makrimenko stated that the critical delay difference depends on the characteristics of the signal such as frequency content and temporal behaviour (Makrinenko, 1986). On the other hand, an echo evaluation method based on the measured impulse response accounts for the ratio between the shift of centre time due to successive reflections and the delay of these reflections (Dietsch and Kraak, 1986). Other scholars based their approach on modulation-transfer function, and they fixed the acoustic conditions required for a certain intelligibility by analysing the modulation of Gregorian chant (D'Orazio *et al.*, 2020; Vitale *et al.*, 2005).

An interesting aspect of spaces with central symmetry with curved sidewalls is the reverberation, even though it is less treated in literature. Tzekakis measured the sound behaviour in the Rotunda of Thessaloniki both in occupied and unoccupied conditions finding optimal listening conditions in the occupied state (Tzekakis, 1975). Furthermore, the acoustic absorption of one surface with respect to the others may affect the sound field (Sumarac-

Pavlovic *et al.*, 2008). Such is the case of mosques (Prodi *et al.*, 2001; Utami, 2004), where almost all of the floor is covered by carpets, or the Byzantine churches (Fausti *et al.*, 2003), due to faithful on the floor and low absorbent walls made of stones all around.

Even though there are several works focused on central-planned curved halls, the role of room modes and free path distribution require further insights. The present paper aims to compensate for this lack, exploiting the opportunity given by wave-based and ray-based numerical models. The former allowed for the analysis of the eigenfrequencies modal density, while the latter permitted the actual distribution of the free path lengths to be calculated. In Section II the workflow is reported, including theoretical hints, a description of the case studies, the acoustic measurements, and the setup of numerical models. Then, Section III provides outcomes along with the consequent remarks and discussions.

II. METHOD

A. Theoretical background

In cylindrical enclosures, the resonant frequencies corresponding to the natural modes have the following general form (Kuttruff, 2016):

$$f(m,n,k) = \frac{c}{2}\sqrt{\left(\frac{\beta_{mn}}{a}\right)^2 + \left(\frac{k}{l_z}\right)^2} \tag{1}$$

where β_{mn} represents the n-th zero of the Bessel function derivative of the first kind of order m (divided by π); a is the radius of the cylinder; l_z is its height. It should be noted that m, n, k are integer numbers ($m = 0, 1, 2, \cdots$; $n = 1, 2, 3, \cdots$; $k = 0, 1, 2, \cdots$) corresponding, respectively, to diametral, circular, and elevation modes. Figure 1 offers a 2D visualization of

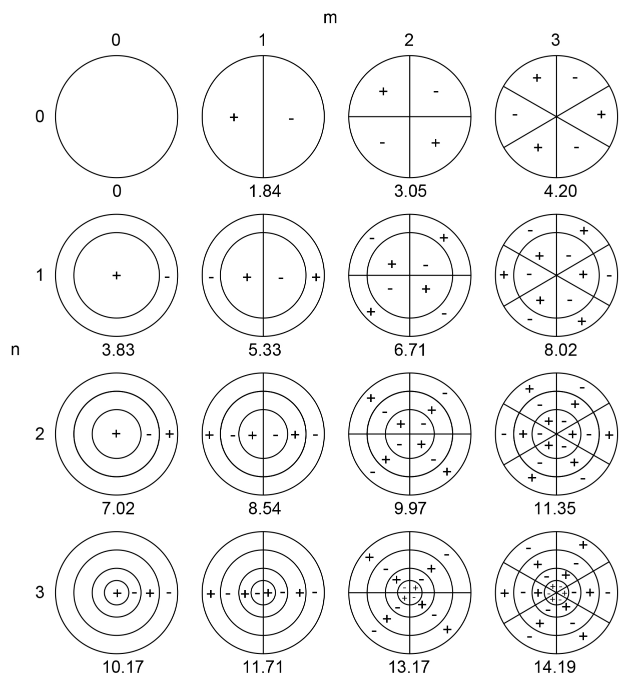

FIG. 1. Nodal lines for transverse pressure distribution in a circular space up to $m = 3, n = 3$ higher order mode. In detail, m is the order of the Bessel function, i.e., the number of pressure nodal diameters, while n is equal to the number of pressure nodal circles (Figure adapted from (Eriksson, 1980)).

m and n in circular spaces up to $m = 3, n = 3$ higher order mode (Eriksson, 1980). According to the conventional notation, $n = 0$ is the first root of $J'_m(k_r a) = 0$ and n is its $(n+1)^{\text{st}}$ root (Lommel, 1868). As the first zero ($n = 0$) of J'_1 is at 1.84 and the second zero ($n = 1$) of J'_0 is at 3.83, the first diametral mode (or azimuthal mode) is at $k_{mn}a = 1.84$, whilst the first circular mode is at $k_{mn}a = 3.83$. When the frequency is low enough ($f < 1.84c/\pi 2a$) or the wavelength is long enough ($\lambda > \pi 2a/1.84$) the wave propagation is that of an unattenuated plane wave ($p(z,t) = [C_1 e^{-jkz} + C_2 e^{+jkz}]e^{+j\omega t}$). In fact, the cut-off frequency for a circular space is:

$$f_{co} = \frac{1.84}{\pi}\frac{c}{2a} = 0.5857\frac{c}{2a}. \tag{2}$$

When the diameter is small, and the signal is centered at low frequencies it is sufficient to perform a 1D analysis to tackle plane wave radiations because Eq. 2 is generally satisfied. Conversely, when it comes to large cylindrical halls, f_{co} significantly drops so that no frequency of interest in room acoustics can be handled with plane waves' propagation laws, and a 3D analysis is required.

The amount of eigenfrequencies in enclosed spaces has been expressed by several scholars that (Blevins, 2006; Bolt *et al.*, 1950; Maa, 1939; Walker, 1996):

$$N_f = \frac{4}{3}\pi V\left(\frac{f}{c}\right)^3 + \frac{\pi}{4}S\left(\frac{f}{c}\right)^2 + \frac{L}{8}\frac{f}{c} \tag{3}$$

where N_f is total number of eigenfrequencies up to the limit frequency f, V is the volume of the hall, S is the total area of all the surfaces, and L is the sum of all edge lengths of the room. The distribution of the resonant frequencies is generally deemed as a continuous function with a reliable approximation because the series of discrete values fluctuate above and below this function (Kinzer and Wilson, 1947). Consequently, the average density of eigenfrequencies at the frequency f is generally equal to

$$\frac{dN}{df} \approx \frac{4\pi V f^2}{c^3} + \frac{\pi S f}{2c^2}. \tag{4}$$

Even though Eqs. 3, 4 have been conceived for rectangular rooms, they are generally valid also for rooms with arbitrary shapes as long as only the first term in the right hand-side of the two equations are considered (Balian and Bloch, 1970; Richardson, 1912). However, they are generally assumed as valid when $f \to \infty$ (Kuttruff, 2016).

B. Case studies

Since early Christianity, round buildings have been frequently used for Baptismal and funerary rituals or by monks for solitary prayer and singing. As a result, Western culture is full of these circular structures, whose shape allows for suitable voice support and intimacy at the same time. Figure 2 shows the three halls taken as case studies: the Odeo Cornaro (OC), the Rotunda Aldini (RA), and the Pisa's Baptistery (PB). The main geometrical and acoustic features of the halls are provided in Table I. Historical references have guided the whole study not only to explore the intended use of the halls but also to infer useful information on the inner materials.

(a) OC (b) RA (c) PB

FIG. 2. (Color online) Interior view of the three well-preserved historical case studies. Courtesy of Reinhard Görner (Fig. 2(a)).

a. Odeo Cornaro (OC). The first case study is a well-preserved Renaissance music space in Padua (Italy). The Odeo Cornaro (OC) is an outstanding Venetian architecture of the 16$^{\text{th}}$ Century designed by the architect Falconetto for the nobleman Alvise Cornaro (Zara,

TABLE I. Details of the nearly cylindrical halls under study. The total volume (V), the radius of the equivalent circular plan (a), the mean height (H), the mean reverberation time value at 500 - 1000 Hz ($T_{30,\mathrm{M}}$), the mean absorption coefficient at 500 - 1000 Hz (α_{M}), the mean sound strength at 500 - 1000 Hz (G_{M}), the Schroeder frequency (f_c), and the number of sound sources (N_S) and receivers (N_R) locations during the measurements are provided for each hall.

Hall ID	V (m^3)	a (m)	H (m)	$T_{30,\mathrm{M}}$ (s)	α_{M}	G_{M} (dB)	f_c (Hz)	N_S	N_R
OC	220	3.3	5.5	2.81	0.05	23	226	2	9
RA	715	4.7	12.2	2.78	0.08	11	125	4	4
PB	23,000	15.6	40.0	13.01	0.03	16	40	3	16

2021). According to the writers of that time (1537-1542), the space was intended to be the music hall of Cornaro's Renaissance mansion. The frequent occurrence of convivial moments with instruments and a choir within the room is explicitly mentioned in the historical report (Moretti, 2010). Since the volume of the hall is moderate (V = 220 m^3), the OC hall was probably reserved for small groups of erudite people only. Historical evidence also states that the hall seemed to significantly support the human voice as the Vitruvius' category of *loci resonantes*. A previous study by the authors concerned the acoustic coupling between the main hall and the surrounding adjacent rooms, along with an insight into the acoustic role of the historical connection doors (Fratoni *et al.*, 2022a).

b. Rotunda Aldini (RA). The second case study is a 12th Century rotunda located in Bologna (Italy). The Rotunda Aldini (RA) was originally built as a central-plan worship space included in a convent complex and it was used as an oratory. Between 1796 and 1802, after its deconsecration, RA hall was incorporated within the lawyer Antonio Aldini's 19th Century villa. The rotunda was preserved and exploited as a music room, located in a larger project that was intended to make the Villa Aldini a place dedicated to arts and culture. In a previous work, the authors acquired a 3D virtual model through a laser scanner and then investigated the acoustic role of the niches by means of finite-difference time-domain methods (Fratoni *et al.*, 2021).

c. Pisa's Baptistery (PB). The third case study is St John's Baptistery in Pisa (Italy). The Baptistery (PB) is an imposing architecture with a cylindrical shape and a conical dome. The ground floor is split into two distinct areas by a circular columns' array: the core of the Baptistery, i.e., the baptismal font, the altar, the pulpit, and the external ambulatory. The upper floor hosts the *matroneum*, a gallery intended to accommodate women, as it is common in ancient worship spaces. The authors previously deepened the archaeoacoustic study of the architecture, with a special focus on its liturgical use (D'Orazio *et al.*, 2020).

C. Acoustic measurements

Between 2017 and 2022, the authors carried out several acoustic surveys to obtain the experimental room acoustics criteria in each case study. The most significant acoustic indicators have been collected in compliance with ISO 3382 (ISO, a). During the measurements, each room was furnished and unoccupied, except for the two operators necessary for the acoustic survey. Impulse responses (IRs) have been acquired using a subwoofer, a high–SPL dodecahedron as an omnidirectional sound source (D'Orazio *et al.*, 2016), a half-inch free-field microphone as a monoaural receiver, a MOTU soundcard, a laptop, and the commercial software Dirac 6.0. Both the sound sources were previously calibrated in a certified reverberation room according to ISO 3741 (ISO, b).

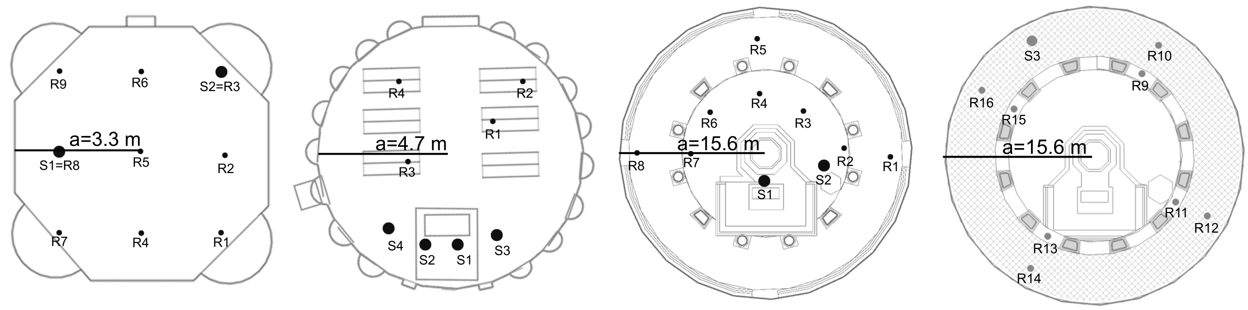

(a) OC (b) RA (c) PB (ground floor) (d) PB (first floor)

FIG. 3. Floor plans indicating the position of sources (S) and receivers (R) in the measurements. The radius of each nearly cylindrical hall is provided (a).

In OC hall, two points were selected for the location of the sound source and a regular grid of nine points was used for the receivers' location (see Fig. 3(a)). The only pieces of furniture were four small benches inside the niches. In RA hall, the sound source was located at four positions behind the altar, corresponding to the places where the singers were supposed to perform in such an oratory/music space. Four locations were selected for the receiver points among the wooden pews present in the rotunda during the measurements (see Fig. 3(b)). In PB hall, the choice of the sound sources and the receivers' location was determined by the spatial distribution of the volumes within the Baptistery. As it is shown in Fig. 3(c), the first two sound source positions on the ground floor - on the altar and on the pulpit - are in line with the liturgical use (Martellotta *et al.*, 2009; Soeta *et al.*, 2012). A third sound source was placed in the *matroneum* to understand the effect of this area on the whole sound field behaviour (see Fig. 3(d)). Three monoaural receivers were placed in the ambulatory, five around the baptismal font and eight in the *matroneum*.

Table I provides the measured reverberation time and sound strength values, along with the derived mean value of the absorption coefficient and the Schroeder frequency for each hall. In this case, data have been averaged between the octave bands centred at 500 Hz and 1000 Hz. Instead, Figure 4 provides the measured T_{30} values in third-octave bands to show its trend at low and mid frequencies (from 80 Hz to 6300 Hz). The box-and-whisker diagram describes the spread of experimental data through a five-number summary: the minimum, the lower quartile, the median, the upper quartile, and the maximum. Where the T_{30} values are comparable, i.e., for OC and RA halls, the same y-axis range has been kept for easier comparison between the halls. Plots show that the spread of T_{30} values is considerably smaller moving forward to higher frequencies. From 1250 Hz onwards the spread turns out to be lower than 10%, 6%, and 5%, respectively, in OC, RA, and PB hall. Moreover, various considerations can be pointed out while comparing the T_{30} spreads of the three case studies. For instance, even though at mid frequencies the experimental reverberation time values of the first two case studies are almost the same (see Table I), OC hall shows a higher mean spread of experimental data (16%) compared to RA hall (4%). This occurs because of the moderate presence of irregular reflections in OC hall (smooth marble, lack of furniture, few niches) compared to RA hall (brick walls, wooden benches, several niches), as can be seen in Fig. 2. In fact, the scattering properties of the surfaces and the edge diffraction contribute

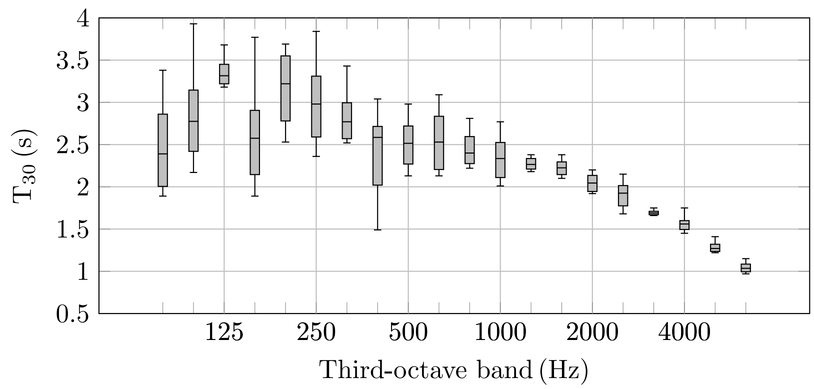

(a) OC

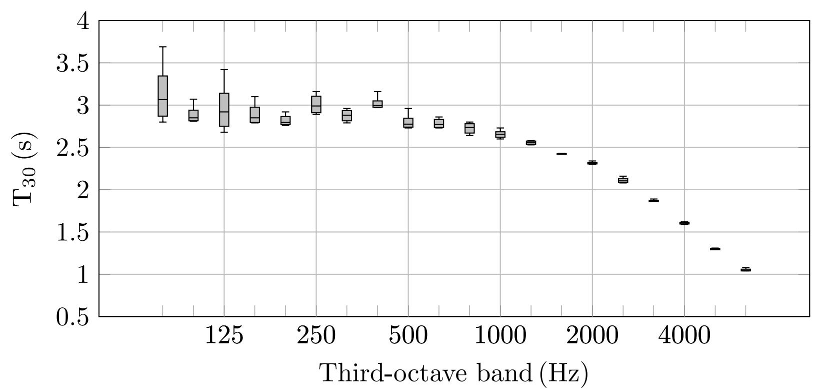

(b) RA

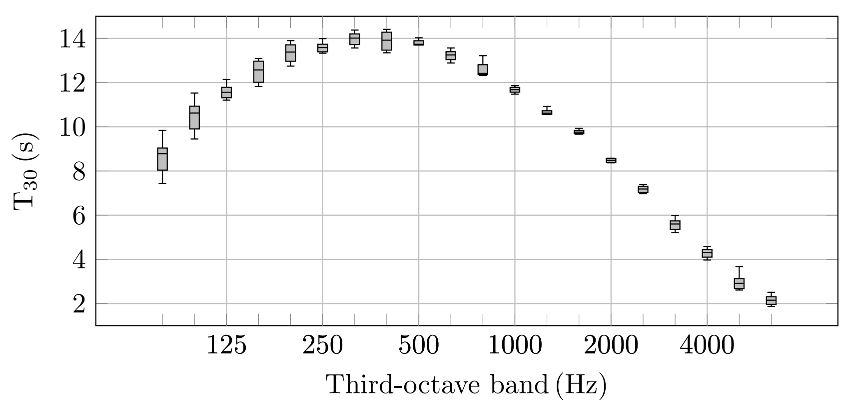

(c) PB

FIG. 4. Measured values of reverberation time (T_{30}) provided in third octave bands in each hall. The minimum, the lower quartile, the median, the upper quartile, and the maximum values are obtained by considering the experimental results of all the source-receiver pairs employed during the measurements.

to increase the sound diffusion and to decrease the spread of experimental data. Moreover, not only OC is the smallest hall among the case studies –and therefore the most affected by modal behaviour–, but also the four rounded corners of the hall plausibly cause focussing effects at the receivers and make the overall shape more similar to a square (see Fig. 3). For this reason, from a global point of view, OC hall shows the highest spread (up to 35% at low frequencies) among the case studies, RA hall shows a moderate spread (up to 17%), and PB hall shows the lowest spread (7% as maximum). This is in line with the expectations, since PB hall has a considerably greater volume compared to OC and RA halls and hosts several columns, altars, and decorations increasing the sound field diffusion (Weber and Katz, 2022).

In the present work, the on-site measurements have been employed not only for derivations of ISO 3382-1 room criteria, but also for calibrating the 3D virtual models of the halls.

D. Numerical models

a. Wave-based models. Recently, wave-based methods have been increasingly used for 3D room acoustics modelling (Fratoni *et al.*, 2022b; Pind *et al.*, 2019; Wang *et al.*, 2019). For the present work, a finite-element (FE) approach has been chosen (Okuzono *et al.*, 2021; Prinn, 2023). As mentioned in Section II A, determining the natural resonant frequencies in real-world geometries is extremely challenging due to the underlying analytical difficulties. COMSOL Multiphysics allowed exploring the modal field at low frequencies in each hall (Maluski and Bougdah, 1997; Tomiku *et al.*, 2008). In particular, the modal density trend has been investigated. The 3D models of OC, RA, and PB halls were built from the scratch in the *Geometry* section of the COMSOL main *Component*, and the resulting models are shown in Fig. 5. A single air domain was defined for each geometry by employing the linear

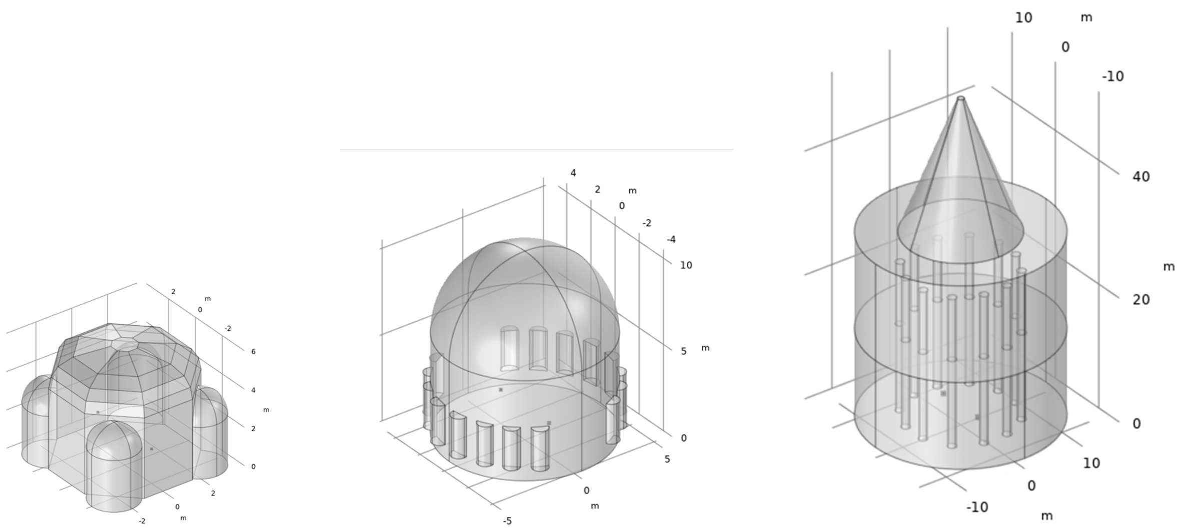

(a) OC (b) RA (c) PB

FIG. 5. View of the 3D finite-element models of the halls under study (COMSOL multiphysics).

elastic model. The atmosphere attenuation can be neglected even in PB hall as long as the analysis is limited to low frequencies. The *Sound Hard Boundary Wall* conditions set on all the surfaces involved are in line with the material features inside the halls: stone, masonry, and marble represent hard and rigid boundary conditions. The mesh of the geometry has been set according to the rule of thumb of 6 elements for the minimum wavelength of interest (Kirkup, 2019). The *Eigenfrequency* study yielded a list of the natural resonance frequencies of each geometry, allowing the calculation of the modal densities (discrete values) for each frequency. The simulation has been run from 80 Hz to around twice the value of each Schroeder frequency to focus on low-frequency behaviour, where natural modes are more detectable and less overlapping.

b. Geometrical Acoustics (GA). Geometrical acoustics (GA) techniques (Odeon Room Acoustics) allowed investigating the free path distribution in the circular places under study (Hidaka and Nishihara, 2006; Naylor, 1993). The 3D virtual models used in previous works by the authors have been exploited for this purpose (D'Orazio *et al.*, 2020; Fratoni *et al.*, 2022a, 2021). During their creation process with Sketchup software, the state-of-art guidelines of 3D modelling have been followed, both in terms of simplification of the actual geometries and the reduction of the details modelled, as it can be seen in Figure 6 (Vorländer, 2020). While a FE calibration at low frequencies would yield various uncertainties due to

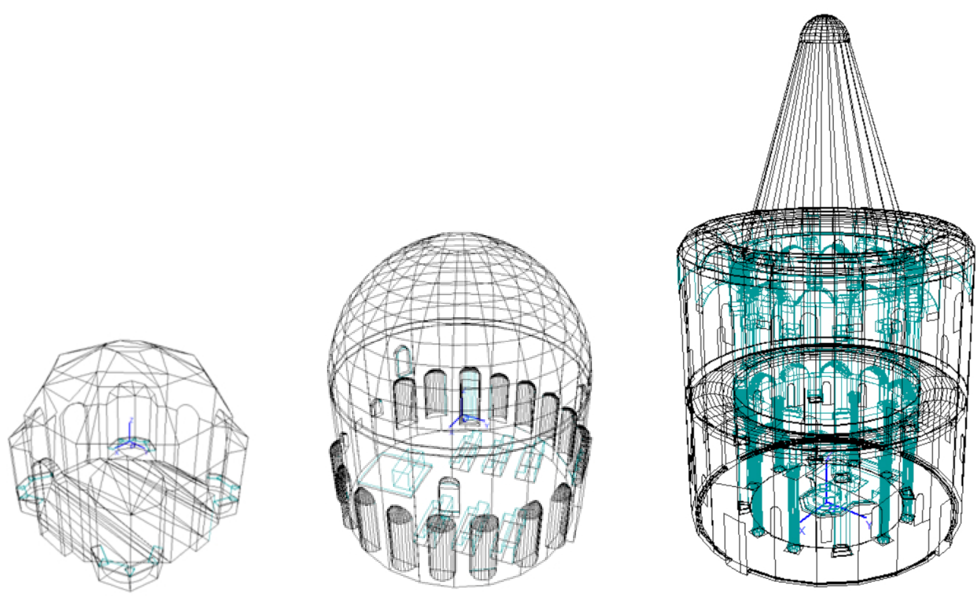

(a) OC (b) RA (c) PB

FIG. 6. View of the GA models under study (Odeon Room Acoustics).

the significant differences between the actual directivity of the dodecahedron and the ideal omnidirectional sound source employed in COMSOL, a complete GA calibration has been achieved according to the state-of-the-art (Pilch, 2020; Postma and Katz, 2016). Table II

TABLE II. Summary of GA calibration: measured and simulated $T_{30,\mathrm{M}}$, EDT_{M}, and $C_{80,\mathrm{M}}$ are provided, along with the corresponding differences. Room criteria have been averaged over the 500 Hz and 1000 Hz octave bands.

	$T_{30,\mathrm{M}}$ (s)			EDT_{M} (s)			$C_{80,\mathrm{M}}$ (dB)		
	Meas.	Sim.	Diff. (%)	Meas.	Sim.	Diff. (%)	Meas.	Sim.	Diff. (dB)
OC	2.74	2.62	4.4%	2.50	2.53	1.2%	-1.7	-1.9	0.2
RA	2.78	2.70	2.7%	2.78	2.71	2.5%	-2.6	-2.2	0.4
PB	12.87	13.25	2.9%	12.61	12.94	2.6%	-12.3	-12.0	0.3

provides a summary of GA calibration by comparing the measured and simulated $T_{30,\mathrm{M}}$, EDT_{M}, and $C_{80,\mathrm{M}}$ values at mid frequencies (500 - 1000 Hz). Those data are provided considering the sound source in S1 (see Fig. 3) and the mean room criteria over all the receiver points.

The ray-tracing tool enabled to determine both the theoretical mean free path according to the classical kinetic theory ($\bar{l}$) and the mean free path evaluated by the simulations ($\bar{l}_{\mathrm{GA}}$) (Prodi and Martellotta, 2014). In the former case the theoretical $\bar{l} = 4V/S$ has been calculated considering the total volume V and the total active surface area S. In the latter case the mean free path ($\bar{l}_{\mathrm{GA}}$) has been obtained by the emission of 200,000 rays for each sound source location, employing the scattering coefficients assigned to the surfaces of the calibrated models.

III. RESULTS AND DISCUSSIONS

A. Eigenfrequencies distribution

The present section reports the simulated modal density distribution obtained through FE simulations in OC, RA, and PB halls. Figure 7 provides the modal densities (discrete values) evaluated by COMSOL with the procedure mentioned in Section II D. The frequency range involves at least $2f_c$ for each case study to include the modal field behaviours (see Table I), and the frequency axis has a linear scale according to the literature (Le Bot, 2015). The Schroeder frequency is also shown with black dashed lines in each case study ($f_{c,OC}$, $f_{c,RA}$, $f_{c,PB}$).

The first analysis concerns the general trend of the graphs. The regression functions of the modal density bars have been derived with a second-degree polynomial function ($dN/df = Af^2+Bf$) through the Curve Fitting Tool by MATLAB to compare the modal density trend obtained through COMSOL and the consolidated assumption (Eq. 4). The consequent regression functions with the corresponding goodness of the fit have been obtained:

- $dN/df = 5.02\pi V f^2/c^3 - 0.08\pi S f/(2c^2)$ with $R^2 = 0.78$ in OC hall,
- $dN/df = 4.18\pi V f^2/c^3 - 1.21\pi S f/(2c^2)$ with $R^2 = 0.80$ in RA hall,
- $dN/df = 3.13\pi V f^2/c^3 + 3.29\pi S f/(2c^2)$ with $R^2 = 0.97$ in PB hall.

Those functions are plotted as dotted curves in the three panes. It is important to highlight that any attempt with linear regression returned lower R^2 values in each model. The difference between the f^2 multiplication factor (A coefficient) and the term $4\pi V/c^3$ in

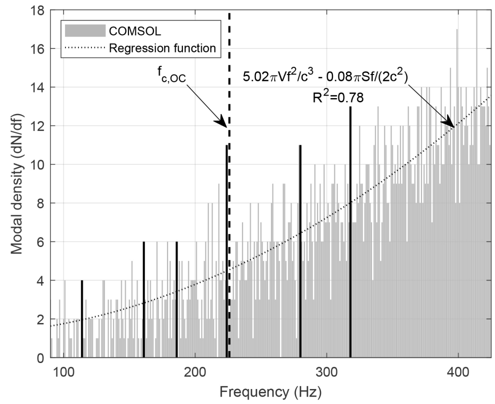

(a) OC

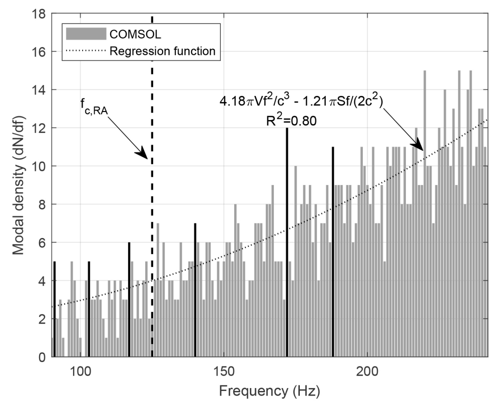

(b) RA

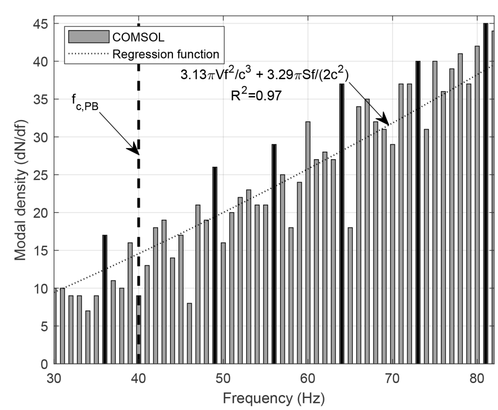

(c) PB

FIG. 7. Simulated eigenfrequencies distribution obtained through COMSOL (frequency bins width 1 Hz). The Schroeder frequency f_c and the regression curve are also shown. The main triplets (m, n, k) corresponding to the peaks of the modal density highlighted in black are provided in Table III.

Eq. 4 is equal to 26% in OC hall, 5% in RA hall, and 22% in PB hall. The difference between the f multiplication factor (B coefficient) and the term $\pi S/(2c^2)$ in Eq. 4 is equal to 92% in OC hall, 21% in RA hall, and 229% in PB hall. The most significant percentage differences could be due to erroneous estimations of the halls' volume, especially in the case of PB hall, which is the largest and the most complex hall under study. The need to simplify the geometries in COMSOL (see Fig. 5) implies unavoidable discrepancies between the actual volumes and the volumes employed during the eigenfrequencies computation. On the other hand, the COMSOL model of the simplest shape, i.e. the RA hall, provides the lowest differences between theoretical and simulated eigenfrequencies distributions. However, apart from the uncertainty related to the volume estimation, the outcomes suggest that the trend of the actual modal density might diverge from the A and B coefficients of Eq. 4 at low frequencies and in central-plan halls.

The second analysis concerns the peaks in eigenfrequencies distributions highlighted in Figure 7. With regard to the theory reported in Section II A, the goal here is to derive the triplets (m, n, k) identifying the natural modes causing modal density peaks at specific frequencies. The procedure of the present study involved the following steps.

1 Since the sound sources (singers, musicians) and the receivers (audience) are placed along a horizontal plane, the attention is focused on the distribution of the modes throughout the circular plans of the halls rather than their elevation. Therefore, in the retrieving calculation of (m, n, k), k values were assumed equal to zero. This assumption allows specifically investigating the prominence of the diametral (m) or the circular (n) modes causing higher modal densities.

TABLE III. List of the first four triplets (m, n, k) identifying the natural modes corresponding to the modal density peaks highlighted in black in Figure 7. The tolerance range between β_{mn} values obtained through Eq. 6 and the tabulated β_{mn} values is below 0.04.

OC	RA	PB
$f = 114\,\mathrm{Hz}$	$f = 91\,\mathrm{Hz}$	$f = 36\,\mathrm{Hz}$
$(0,2,0)$ $(2,2,0)$ $(5,1,0)$ $(6,1,0)$	$(0,2,0)$ $(1,3,0)$ $(3,2,0)$ $(6,1,0)$	$(0,3,0)$ $(2,3,0)$ $(5,2,0)$ $(3,3,0)$
$f = 161\,\mathrm{Hz}$	$f = 103\,\mathrm{Hz}$	$f = 49\,\mathrm{Hz}$
$(0,3,0)$ $(4,2,0)$ $(2,3,0)$ $(5,2,0)$	$(1,3,0)$ $(2,3,0)$ $(4,2,0)$ $(7,1,0)$	$(0,4,0)$ $(1,5,0)$ $(2,4,0)$ $(3,4,0)$
$f = 186\,\mathrm{Hz}$	$f = 117\,\mathrm{Hz}$	$f = 56\,\mathrm{Hz}$
$(1,4,0)$ $(3,3,0)$ $(6,2,0)$ $(9,1,0)$	$(0,3,0)$ $(2,3,0)$ $(4,2,0)$ $(5,2,0)$	$(0,5,0)$ $(2,5,0)$ $(4,4,0)$ $(6,3,0)$
$f = 224\,\mathrm{Hz}$	$f = 140\,\mathrm{Hz}$	$f = 64\,\mathrm{Hz}$
$(0,4,0)$ $(2,4,0)$ $(4,3,0)$ $(7,2,0)$	$(1,4,0)$ $(3,3,0)$ $(4,3,0)$ $(6,2,0)$	$(1,6,0)$ $(3,5,0)$ $(5,4,0)$ $(6,4,0)$
$f = 280\,\mathrm{Hz}$	$f = 172\,\mathrm{Hz}$	$f = 73\,\mathrm{Hz}$
$(0,5,0)$ $(2,5,0)$ $(5,4,0)$ $(7,3,0)$	$(1,5,0)$ $(3,4,0)$ $(6,3,0)$ $(8,2,0)$	$(1,7,0)$ $(3,6,0)$ $(5,5,0)$ $(8,4,0)$
$f = 318\,\mathrm{Hz}$	$f = 180\,\mathrm{Hz}$	$f = 81\,\mathrm{Hz}$
$(0,6,0)$ $(4,5,0)$ $(2,6,0)$ $(6,4,0)$	$(0,5,0)$ $(2,5,0)$ $(4,4,0)$ $(7,3,0)$	$(0,7,0)$ $(2,7,0)$ $(5,6,0)$ $(7,5,0)$

2 The inverse function of Eq. 1 has been used to obtain the triplets $(m, n, 0)$ corresponding to the n$-th$ roots of the Bessel function derivatives (J'_m) of order m. Accounting for the assumption aforementioned $(k = 0)$, Eq. 1 becomes:

$$f(m, n, 0) = \frac{c\beta_{mn}}{2a} \tag{5}$$

where $\beta_{mn}\pi$ are the roots of the Bessel function derivative of the first kind of order m (listed through MATLAB in this work). For each frequency interested by modal density peaks (f_{peak}), the corresponding $(m, n, 0)$ has been found as follows:

$$\beta_{mn} = \frac{2a}{c} f_{peak} \Rightarrow (m, n, 0). \tag{6}$$

The tolerance range between the values obtained through Eq. 6 and the tabulated values has been kept below 0.04.

Table III provides the first four triplets $(m, n, 0)$ corresponding to each f_{peak} assessed. It is possible to notice that in the first pair of triplets, n index assumes higher values than m for most of the cases (92% of the pairs). This may suggest a stronger prominence of circular modes compared to the diametral ones.

B. Free path distribution

The present section reports the free path distribution resulting from Odeon in each case study, using the scattering coefficients assigned to the surfaces in the materials list. Figure 8 provides the results in terms of the normalised frequency of surface hits versus the length of free paths in meters, derived from the study of 200,000 rays. The y-axis has been normalised

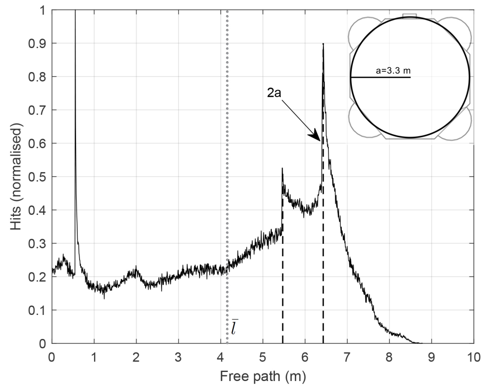

(a) OC

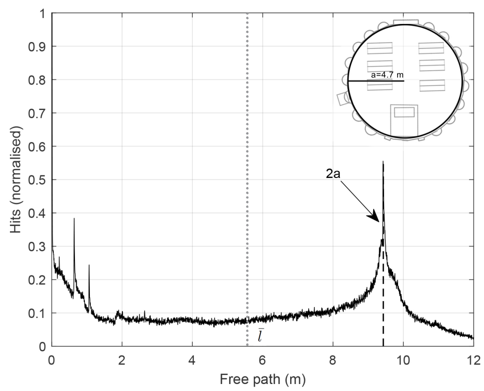

(b) RA

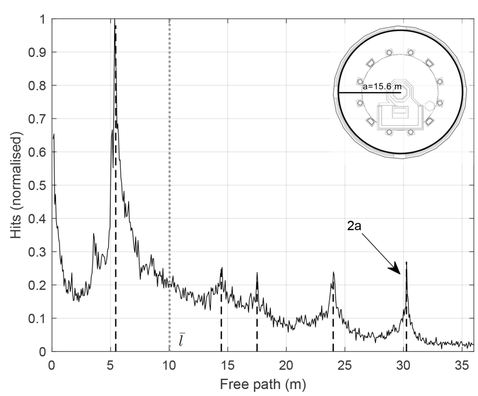

(c) PB

FIG. 8. Normalised frequency of surface hits versus the distance of free paths in meters in OC, RA, and PB hall obtained with 200,000 rays (Odeon). The prominent paths are highlighted in each geometry with dashed lines while $\bar{l} = 4V/S$ is plotted as a gray dotted line.

by dividing each number of hits by the maximum value, obtaining sets of values ranging from 0 and 1. The normalised distributions show that the highest probabilities correspond to the shortest path lengths in the proximity of zero, in line with previous studies (Beranek and Nishihara, 2014; Hidaka and Nishihara, 2006; Kuttruff, 2016; Ŝumarac-Pavlović and Mijić, 2007). In OC hall, the highly recurrent 0.8 m path is due to the curved surfaces discretisation, as 0.8 m corresponds to the size of the segments composing each niche. A different issue is the almost zero length paths in RA hall (0.01 m) and PB hall (0.10 m) because there are no details of that dimension in the 3D models. A possible explanation is the accumulation of short path reflections in the proximity of all the corners of the 3D models. Moreover, it is plausible that discrete approaches assume a lower limit for the distance resolution to avoid the distribution from diverging in the vicinity of zero (Krämer, 1997). Apart from such recurrent short path lenghts, the main prominent paths are highlighted in each geometry with dashed lines while $\bar{l} = 4V/S$ is plotted as a gray dotted line. It is possible to notice the prominence of the diameter ($2a$) of the halls in each case (6.6 m in OC hall, 9.4 m in RA hall, and 30.2 m in PB hall) confirming the strong influence of the circular plan on the preferred paths. However, further considerations are required for the single cases.

1 In OC hall, with the exception of the first peak at 0.8 m, the second peak at 5.5 m is clearly visible in the distribution. This corresponds to the dimension of the height of the room. However, in that case, the normalised number of hits is almost halved compared to the diameter of the hall (6.6 m), confirming again the stronger influence on the sound propagation of the circular shape compared to the elevation size.

2 In RA hall, the diameter size (9.4 m) represents the only neat peak in the whole distribution of the hits occurrences. This can be due to the spherical shape of the dome which significantly reduces the probability of further prominent paths.

3 In PB hall, the highest peak corresponds to the ambulatory width (5.4 m), highlighting a prominence of the annular space between the sidewalls and the columns for the preferred paths. Right after 5.4 m, the diameter (30.2 m) is the distance with the highest number of hits, followed by 24 m, which is the height of the conical dome, and 14 m, which is the height of each floor. Thus, PB exhibits multimodal effects not shown by the other two halls.

Furthermore, insights into the mean free path in circular halls are here reported. In room acoustics, calculating the predicted reverberation time requires the formula for the mean free path, i.e., the average distance between two successive impacts of sound "rays" on the walls (Kingman, 1965; Kosten, 1960). Generally, the formula used in the kinetic theory of gases is employed: $\bar{l} = 4V/S$, where V is the volume of the room and S is the total internal surface area of the room (Jaeger, 1911). On diffuse field assumption, this formula is supposed to be independent of the shape of the hall under study. However, in the late 1920s and the first years of the 1930s, approximated formulas were developed for cubic, cylindrical, and spherical shapes (Schuster and Waetzmann, 1929), as follows:

- $\bar{l}_{\text{cub}} = 2\sqrt{3}\text{V/S}$ for the cubic shape;
- $\bar{l}_{\text{cyl}} = 3\sqrt{2}V/S$ for the cylindrical shape (corresponding to 4.3 m for OC hall, 5.9 m for RA hall, 10.6 m for PB hall);

TABLE IV. Comparison between the mean free paths calculated according to the classical kinetic theory ($\bar{l} = 4V/S$) (Bate and Pillow, 1947; Jaeger, 1911), depending on the cylindrical shape ($\bar{l}_{\text{cyl}} = 3\sqrt{2}V/S$) (Schuster and Waetzmann, 1929), and obtained with geometrical acoustics simulations (Naylor, 1993). The mean free path and the relative variance are provided for three simulated scenarios: "Calibrated models" ($\bar{l}_{\text{GA}}$, γ^2_{GA}) where each layer has his own set of adequate scattering coefficients, "Scattering 1" where all the surfaces have $s = 1$ ($\bar{l}_{\text{GA,1}}$, $\gamma^2_{\text{GA,1}}$), "Scattering 0" where all the surfaces have $s = 0$ ($\bar{l}_{\text{GA,0}}$, $\gamma^2_{\text{GA,0}}$) (Kuttruff, 2016).

			Calibrated models		Scattering 1		Scattering 0	
	$\frac{4V}{S}$	$\frac{3\sqrt{2}V}{S}$	$\bar{l}_{\text{GA}}$	γ^2_{GA}	$\bar{l}_{\text{GA,1}}$	$\gamma^2_{\text{GA,1}}$	$\bar{l}_{\text{GA,0}}$	$\gamma^2_{\text{GA,0}}$
OC	4.1 m	4.3 m	4.3 m	0.26	3.8 m	0.39	4.2 m	0.27
RA	5.6 m	5.9 m	5.8 m	0.39	5.3 m	0.49	5.8 m	0.39
PB	10.0 m	10.6 m	11.9 m	0.61	10.8 m	0.69	11.6 m	0.61

- $\bar{l}_{\text{sph}} = 6V/S$ for the spherical shape.

Later, experimental results proved again that a good approximation for usual rooms is $\bar{l} = 4V/S$ regardless of the shape of the rooms (Knudsen, 1932). The same outcomes were achieved by the direct averaging of mean free paths in rectangular, spherical, and cylindrical enclosures (Bate and Pillow, 1947). It is interesting to notice that up that time the scattering influence on the mean free path is not explicitly mentioned in the literature. Then, Joyce demonstrated that $\bar{l} = 4V/S$ is valid in case of sound field diffusion and that the circular shape assists the randomizing effect of any amount of scattering (Joyce, 1975, 1978). Beranek and Nishihara's outcomes show that in almost all the concert halls $\bar{l} = 4V/S$, except for the hall with an "unusual shape" (Beranek and Nishihara, 2014). According to Kuttruff's findings, the shape of the room and the preferred sound paths affect the way the actual free path lengths are distributed around their mean (Kuttruff, 2016). With this regard, a useful indicator is the relative variance of free path lengths, expressed as:

$$\gamma^2 = \frac{\sigma^2}{\bar{l}^2} \tag{7}$$

where σ^2 and $\bar{l}$ are, respectively, the variance and the mean value of the free path lengths. Generally, γ^2 can be calculated directly only for a limited number of geometries, e.g., for a sphere ($\gamma^2 = 1/8 = 0.125$). Even though most of the shapes return $\gamma^2 \approx 0.4$, specific shapes require acoustic simulation to determine γ^2 values (Kuttruff, 2016).

In the present study, Odeon's ray-tracing algorithm has been employed also with such purpose. The outcomes obtained with the method described in Section II D are provided in Table IV in terms of experienced $\bar{l}_{\mathrm{GA}}$ and the relative variance γ^2_{GA} in each hall, considering the scattering coefficients used to calibrate the model (Kuttruff, 2016). Such values are compared with the mean free paths calculated according to the classical kinetic theory ($\bar{l} = 4V/S$) (Bate and Pillow, 1947; Jaeger, 1911) and depending on the cylindrical shape ($\bar{l}_{\mathrm{cyl}} = 3\sqrt{2}V/S$) (Schuster and Waetzmann, 1929). From the comparison between the mean free paths provided by Table IV, it is possible to notice than the ratios $\bar{l}_{\mathrm{GA}}/\bar{l}$ assume higher values (≈ 1.05) than the ratios $\bar{l}_{\mathrm{GA}}/\bar{l}_{\mathrm{cyl}}$ (≈ 1) (Hidaka and Nishihara, 2006). Therefore, the values obtained through the ray-tracing method are more similar to the values depending on the cylindrical shape of the halls rather than the classical kinetic theory (Stephenson, 2012). The lowest relative variance is $\gamma^2_{\mathrm{GA}} = 0.26$ in OC hall; a value of $\gamma^2_{\mathrm{GA}} = 0.39$ has been found in RA hall; and the highest value experienced in this work is $\gamma^2_{\mathrm{GA}} = 0.60$ in PB hall, in accordance with numerical experiments (Kuttruff, 2016).

Moreover, the mean free path and the relative variance are provided for two further simulated scenarios: "Scattering 1" with $s = 1$ assigned to all the surfaces ($\bar{l}_{\mathrm{GA,1}}$, $\gamma^2_{\mathrm{GA,1}}$), and "Scattering 0" with $s = 0$ assigned to all the surfaces ($\bar{l}_{\mathrm{GA,0}}$, $\gamma^2_{\mathrm{GA,0}}$). In all the case studies assessed, the difference between the real-world scenarios corresponding to "Calibrated models" and the "Scattering 0" scenario is neglectable ($< 2\%$), whilst the "Scattering 1" scenario yields $\bar{l}_{\mathrm{GA,1}}$ values 8%-11% lower than $\bar{l}_{\mathrm{GA}}$, $\bar{l}_{\mathrm{GA,0}}$, and $\gamma^2_{\mathrm{GA,1}}$ values 10%-30% higher than γ^2_{GA}, $\gamma^2_{\mathrm{GA,0}}$. Finally, the reverberation time related to the plausible condition of the calibrated models, i.e. assuming $\bar{l}_{\mathrm{GA}}$ as realistic mean free path, is expressed as:

$$T = \frac{-6\ln 10}{c}\frac{\bar{l}_{\mathrm{GA}}}{\ln(1-\alpha)} \approx 0.04\frac{\bar{l}_{\mathrm{GA}}}{\alpha} \quad [s], \tag{8}$$

implying that a longer $\bar{l}_{\mathrm{GA}}$ suggests longer reverberation time values in circular halls compared to rectangular halls with the same volume (Hidaka and Nishihara, 2006).

IV. CONCLUSIONS

The present work investigates the acoustics of circular ancient halls, based on measured data and numerical models. The experimental results permitted to obtain information about the amount of diffusing surfaces and the influence of the modal behaviour through the assessment of T_{30} values spread in third-octave bands at mid and low frequencies. Notwithstanding the similar mean value of reverberation time at mid frequencies in OC and RA halls, the significantly higher mean spread of T_{30} in OC hall (16%) than in RA hall (4%) suggests uneven room acoustics criteria in the former hall. This can be related to several OC's features, such as the moderate presence of diffusing surfaces, the small size, and the plausible focussing effects caused by the four rounded corners. Then, from the eigenfrequencies distributions obtained with COMSOL, it has been found a strong relationship between the peaks of modal density and the circular modes rather than the diametral or elevation modes ($n > m$ in $f_{peak}(m, n, 0)$, assuming $k = 0$). Moreover, the analysis of the free path distribution through geometrical acoustics confirmed the importance of the circular shape on the horizontal plane, as the diameter size is generally the most recurrent free path. With this regard, the PB hall represents an exception because it has a more composite geometry with also a significant influence of the annular resonance of the ambulatory between the sidewalls and the columns. Finally, similar to what has been found in previous works, the general trend of the ratio $\bar{l}_{\mathrm{GA}}/\bar{l}$ is higher than 1 in each case study, suggesting longer reverberation time values compared to halls with other shapes and the same volume. Therefore, the circular environments proved to adequately support the sound signals, as it was mentioned in the historical reports taken as references.

ACKNOWLEDGMENTS

The authors would like to thank Anna Rovigatti, Domenico De Salvio, Elena Rossi, Riccardo Russo, Michele Ducceschi, and Virginia Tardini for their kind support during the acoustic measurements.

AUTHOR DECLARATIONS

Conflict of Interest

The authors have no conflicts to disclose.

Ethics Approval

No human subjects or animals were involved in the research.

DATA AVAILABILITY

The data that support the findings of this study are available from the corresponding author.

(a). *ISO 3382-1:2009 Acoustics — Measurement of room acoustic parameters.*

(b). *ISO 3741:2010 Acoustics — Determination of sound power levels and sound energy levels of noise sources using sound pressure — Precision methods for reverberation test rooms.*

Alberdi, E., Martellotta, F., Galindo, M., and León, Á. L. (**2019**). "Dome sound effect in the church of san luis de los franceses," Applied Acoustics **156**, 56–65.

Balian, R., and Bloch, C. (**1970**). "Distribution of eigenfrequencies for the wave equation in a finite domain: I. three-dimensional problem with smooth boundary surface," Annals of Physics **60**(2), 401–447.

Bate, A. (**1938**). “Note on the whispering gallery of St Paul’s Cathedral, London,” Proceedings of the Physical Society (1926-1948) **50**(2), 293.

Bate, A., and Pillow, M. (**1947**). “Mean free path of sound in an auditorium,” Proceedings of the Physical Society (1926-1948) **59**(4), 535.

Beranek, L. L., and Nishihara, N. (**2014**). “Mean-free-paths in concert and chamber music halls and the correct method for calibrating dodecahedral sound sources,” The Journal of the Acoustical Society of America **135**(1), 223–230.

Blevins, R. (**2006**). “Modal density of rectangular volumes, areas, and lines,” The Journal of the Acoustical Society of America **119**(2), 788–791.

Bolt, R., Doak, P., and Westervelt, P. (**1950**). “Pulse statistics analysis of room acoustics,” The Journal of the Acoustical Society of America **22**(3), 328–340.

Cremer, L., and Müller, H. A. (**1978**). *Die wissenschaftlichen Grundlagen der Raumakustik* (Hirzel Stuttgart).

D. D’Orazio, A. Rovigatti, M. G. (**2019**). “The proscenium of opera houses as a disappeared intangible heritage: a virtual reconstruction of the 1840s original design of the Alighieri Theatre in Ravenna,” in *Acoustics*, Multidisciplinary Digital Publishing Institute, Vol. 1, pp. 694–710.

Dietsch, L., and Kraak, W. (**1986**). “Ein objektives Kriterium zur Erfassung von Echostörungen bei Musik-und Sprachdarbietungen,” Acta Acustica United with Acustica **60**(3), 205–216.

D’Orazio, D., De Cesaris, S., Guidorzi, P., Barbaresi, L., Garai, M., and Magalotti, R. (**2016**). “Room acoustic measurements using a high SPL dodecahedron,” in *Audio Engi-*

neering Society Convention 140, Audio Engineering Society.

D'Orazio, D., Fratoni, G., Rossi, E., and Garai, M. (**2020**). "Understanding the acoustics of St. John's Baptistery in pisa through a virtual approach," Journal of Building Performance Simulation **13**(3), 320–333.

Eriksson, L. J. (**1980**). "Higher order mode effects in circular ducts and expansion chambers," The Journal of the Acoustical Society of America **68**(2), 545–550.

Fausti, P., Pompoli, R., and Prodi, N. (**2003**). "Comparing the acoustics of mosques and byzantine churches," in *19th International Symposium CIPA*, Citeseer.

Fratoni, G., D'Orazio, D., Ducceschi, M., and Garai, M. (**2022**a). "The coupled rooms of Odeo Cornaro (1534) as support for Renaissance musicians and soloists," in *Proceedings of the 24th International Congress on Acoustics.*

Fratoni, G., Hamilton, B., and D'Orazio, D. (**2022**b). "Feasibility of a finite-difference time-domain model in large-scale acoustic simulations," The Journal of the Acoustical Society of America **152**(1), 330–341.

Fratoni, G., Hamilton, B., and D'Orazio, D. (**2021**). "Rediscovering the acoustics of a XII-Century Rotunda through FDTD simulation," in *2021 Immersive and 3D Audio: from Architecture to Automotive (I3DA)*, IEEE, pp. 1–8.

Haas, H. (**1951**). "Über den Einfluβ eines Einfachechos auf die Hörsamkeit von Sprache," Acta Acustica united with Acustica **1**(2), 49–58.

Hidaka, T., and Nishihara, N. (**2006**). "Reverberation time, mean-free-path, and sound absorption in concert halls—numerical examination by computer simulation," The Journal of the Acoustical Society of America **119**(5_Supplement), 3430–3430.

Jaeger, G. (**1911**). "Zur Theorie des Nachhalls.," Sitzungsebr. Wiener Akad. **Kl. 120**(IIa), 613–634.

Joyce, W. (**1975**). "Sabine's reverberation time and ergodic auditoriums," The Journal of the Acoustical Society of America **58**(3), 643–655.

Joyce, W. (**1978**). "Exact effect of surface roughness on the reverberation time of a uniformly absorbing spherical enclosure," The Journal of the Acoustical Society of America **64**(5), 1429–1436.

Kingman, J. (**1965**). "Mean free paths in a convex reflecting region," Journal of Applied Probability **2**(1), 162–168.

Kinzer, J., and Wilson, I. (**1947**). "Some results on cylindrical cavity resonators," Bell System Technical Journal **26**(3), 410–445.

Kircher, A. (**1673**). *Phonurgia nova sive conjugium mechanicophysicum artis et naturae paranympha phonosophia concinnatum (etc.)* (Dreherr).

Kirkup, S. (**2019**). "The boundary element method in acoustics: A survey," Applied Sciences **9**(8), 1642.

Knudsen, V. O. (**1932**). *Architectural acoustics.* (Wiley).

Kosała, K., and Małecki, P. (**2018**). "Index assessment of the acoustics of orthodox churches in poland," Applied Acoustics **130**, 140–148.

Kosten, C. (**1960**). "The mean free path in room acoustics," Acta Acustica united with Acustica **10**(4), 245–250.

Krämer, P. S. (**1997**). "Mean free path length for radiating point sources in specular reflecting enclosures," Acta Acustica united with Acustica **83**(4), 629–634.

Kuttruff, H. (**2016**). *Room acoustics* (Crc Press).

Le Bot, A. (**2015**). *Foundation of statistical energy analysis in vibroacoustics* (OUP Oxford).

Lommel, E. (**1868**). *Studien über die Bessel'schen Functionen* (BG Teubner).

Maa, D.-Y. (**1939**). "Distribution of eigentones in a rectangular chamber at low frequency range," The Journal of the Acoustical Society of America **10**(3), 235–238.

Maa, D.-Y. (**1941**). "The flutter echoes," The Journal of the Acoustical Society of America **13**(2), 170–178.

Magrini, A., and Ricciardi, P. (**2006**). "The acoustic field under the dome in a central plan church: measurement and simulation," Proc 13th ICSV, Vienna, Austria 2–6.

Makrinenko, L. (**1986**). "Acoustics of public buildings," Moskva: Stroyizdat. Revision of the literature on building materials and structures **173**.

Maluski, S., and Bougdah, H. (**1997**). "Predicted and measured low frequency response of small rooms," Building Acoustics **4**(2), 73–86.

Martellotta, F., Cirillo, E., Carbonari, A., and Ricciardi, P. (**2009**). "Guidelines for acoustical measurements in churches," Applied Acoustics **70**(2), 378–388.

Meyer, H. B. (**1964**). "Acoustics and people," The Journal of the Acoustical Society of America **36**(10), 1967–1968.

Moreno, A., Zaragoza, J. G., and Alcantarilla, F. (**1981**). "Generation and suppression of flutter echoes in spherical domes," Journal of the Acoustical Society of Japan (E) **2**(4), 197–202.

Moretti, L. (**2010**). "Quivi si essercitaranno le musiche: La sala della musica presso la corte padovana di Alvise Cornaro," Music in Art 135–144.

Muncey, R., Nickson, A., and Dubout, P. (**1953**). "The acceptability of speech and music with a single artificial echo," Acta Acustica united with Acustica **3**(3), 168–173.

Naylor, G. M. (**1993**). "Odeon—another hybrid room acoustical model," Applied Acoustics **38**(2-4), 131–143.

Okuzono, T., Yoshida, T., and Sakagami, K. (**2021**). "Efficiency of room acoustic simulations with time-domain fem including frequency-dependent absorbing boundary conditions: Comparison with frequency-domain FEM," Applied Acoustics **182**, 108212.

Petzold, E. (**1930**). "Sounding surfaces," The Journal of the Acoustical Society of America **2**(2), 305–308.

Pilch, A. (**2020**). "Optimization-based method for the calibration of geometrical acoustic models," Applied Acoustics **170**, 107495.

Pind, F., Engsig-Karup, A. P., Jeong, C.-H., Hesthaven, J. S., Mejling, M. S., and Strømann-Andersen, J. (**2019**). "Time domain room acoustic simulations using the spectral element method," The Journal of the Acoustical Society of America **145**(6), 3299–3310.

Postma, B. N., and Katz, B. F. (**2016**). "Perceptive and objective evaluation of calibrated room acoustic simulation auralizations," The Journal of the Acoustical Society of America **140**(6), 4326–4337.

Prinn, A. G. (**2023**). "A review of finite element methods for room acoustics," in *Acoustics*, MDPI, Vol. 5, pp. 367–395.

Prodi, N., Marsilio, M., and Pompoli, R. (**2001**). "On the prediction of reverberation time and strength in mosques," Proceedings of the 17th ICA, Rome .

Prodi, N., and Martellotta, F. (**2014**). "On the statistical properties of free path distribution as a means to investigate room acoustics of theatre halls," in *Proceedings of Forum Acusticum 2014*, pp. 8–12.

Reichardt, W. (**1968**). "Der Impuls-Schalltest und seine raumakustische Beurteilung," Proc. 6th Int. Congr. Acoustics, Tokyo, 1968 .

Richardson, R. (**1912**). "Theorems of oscillation for two linear differential equations of the second order with two parameters," Transactions of the American Mathematical Society **13**(1), 22–34.

Sabine, W. (**1922**). "Whispering galleries," Collected Papers on Acoustics. Cambridge, MA: Harvard University Press .

Schuster, K., and Waetzmann, E. (**1929**). "Über den Nachhall in geschlossenen Räumen," Annalen der Physik **393**(5), 671–695.

Shepherd, M., Leishman, T. W., and Utami, S. (**2005**). "Acoustics of a planetarium," The Journal of the Acoustical Society of America **118**(3), 1999–1999.

Soeta, Y., Ito, K., Shimokura, R., Sato, S.-i., Ohsawa, T., and Ando, Y. (**2012**). "Effects of sound source location and direction on acoustic parameters in Japanese churches," The Journal of the Acoustical Society of America **131**(2), 1206–1220.

Stephenson, U. M. (**2012**). "Different assumptions-different reverberation formulae," in *INTER-NOISE and NOISE-CON Congress and Conference Proceedings*, Institute of Noise Control Engineering, Vol. 2012, pp. 7646–7657.

Sü Gül, Z., Xiang, N., and Çalışkan, M. (**2016**). "Investigations on sound energy decays and flows in a monumental mosque," The Journal of the Acoustical Society of America

140(1), 344–355.

Ŝumarac-Pavlović, D., and Mijić, M. (**2007**). “An insight into the influence of geometrical features of rooms on their acoustic response based on free path length distribution,” Acta Acustica united with Acustica **93**(6), 1012–1026.

Sumarac-Pavlovic, D., Mijic, M., and Kurtovic, H. (**2008**). “A simple impulse sound source for measurements in room acoustics,” Applied Acoustics **69**(4), 378–383.

Tomiku, R., Otsuru, T., Okamoto, N., and Kurogi, Y. (**2008**). “Direct and modal frequency response analysis of sound fields in small rooms by finite element method,” Journal of the Acoustical Society of America **123**(5), 3092.

Tzekakis, E. G. (**1975**). “Reverberation time of the rotunda of Thessaloniki,” The Journal of the Acoustical Society of America **57**(5), 1207–1209.

Utami, S. S. (**2004**). “An acoustical analysis of a room with a concave dome ceiling element,” The Journal of the Acoustical Society of America **115**(5), 2581–2581.

Vitale, R., Pisani, R., Onali, P., and Astolfi, A. (**2005**). “Why does the acoustic space of churches exalt Gregorian chant?,” in *Proceedings of the 31th International Computer Music Conference (ICMC), Barcelona, Spain, September*, pp. 4–10.

Vorländer, M. (**2020**). *Auralization* (Springer).

Walker, R. (**1996**). “Room modes and low-frequency responses in small enclosures,” in *Audio Engineering Society Convention 100*, Audio Engineering Society.

Wang, H., Sihar, I., Pagán Muñoz, R., and Hornikx, M. (**2019**). “Room acoustics modelling in the time-domain with the nodal discontinuous Galerkin method,” The Journal of the Acoustical Society of America **145**(4), 2650–2663.

Weber, A., and Katz, B. F. (**2022**). “Sound Scattering by Gothic Piers and Columns of the Cathédrale Notre-Dame de Paris,” in *Acoustics*, Multidisciplinary Digital Publishing Institute, Vol. 4, pp. 679–703.

Zara, V. (**2021**). “Music, architecture, proportion and the renaissance way of thinking,” European Review **29**(2), 226–241.